

## An analytical solution of coagulation processes with collision-induced fragmentation

This article has been downloaded from IOPscience. Please scroll down to see the full text article.

2008 J. Phys. A: Math. Theor. 41 285005

(<http://iopscience.iop.org/1751-8121/41/28/285005>)

View [the table of contents for this issue](#), or go to the [journal homepage](#) for more

Download details:

IP Address: 171.66.16.149

The article was downloaded on 03/06/2010 at 06:58

Please note that [terms and conditions apply](#).

# An analytical solution of coagulation processes with collision-induced fragmentation

Jianhong Ke<sup>1,2</sup>, Zhenquan Lin<sup>1</sup> and Xiaoshuang Chen<sup>2</sup>

<sup>1</sup> School of Physics and Electronic Information, Wenzhou University, Wenzhou 325027, People's Republic of China

<sup>2</sup> National Laboratory of Infrared Physics, Shanghai Institute of Technical Physics, Chinese Academy of Sciences, Shanghai 200083, People's Republic of China

E-mail: [kejianhong@yahoo.com.cn](mailto:kejianhong@yahoo.com.cn) and [xschen@mail.sitp.ac.cn](mailto:xschen@mail.sitp.ac.cn)

Received 26 March 2008, in final form 6 May 2008

Published 19 June 2008

Online at [stacks.iop.org/JPhysA/41/285005](http://stacks.iop.org/JPhysA/41/285005)

## Abstract

We propose a single-species coagulation model with collision-induced fragmentation, in which a pair of clusters can coagulate into a larger one if their encounter is a complete inelastic collision; otherwise, one of them will fragment into two smaller clusters due to a destructive collision. Consider a simple system with the constant coagulation kernel  $I(i, j) = I$  and the size-dependent fragmentation kernel  $J(l; i, j) = 2Jl^u$ . We then investigate analytically the kinetic behavior of such a system by means of the rate-equation approach. It is indicated that the results are crucially dependent on the value of index  $u$ . In the case of  $u < -1$  and  $I \geq 2J\zeta(-u)$  (here  $\zeta(x)$  is the Riemann zeta function), the cluster size distribution  $a_k(t)$  approaches the conventional scaling form, and the system will evolve permanently in time. While in other cases,  $a_k(t)$  always takes the modified scaling form; moreover, a balance can be established between coagulation and collision-induced breakage processes, and thus the system can eventually evolve to a steady state.

PACS numbers: 82.20.-w, 68.43.Jk, 82.30.Lp, 89.75.Da

(Some figures in this article are in colour only in the electronic version)

## 1. Introduction

Irreversible coagulation processes are central to a wide range of theoretical and applied fields and have thus attracted a considerable amount of interest [1–10]. While in some practical situations, the reverse process of coagulation (namely, fragmentation of clusters) also plays an important role in the dynamic evolution of cluster growth [11–16]. Fragmentation can be classified into two categories. If fragmentation of a cluster is driven only by a homogenous external agent, such processes are inherently linear, namely, the fragmentation rate of a  $k$ -mer (namely, a cluster consisting of  $k$  monomers) can be assumed to be proportional to the

concentration of  $k$ -mers [14]. If interactions between fragments are essential, such processes are intrinsically nonlinear [16]. Coagulation and fragmentation processes are ubiquitous in nature and are thus of great importance. Examples include reversible colloidal aggregation, polymer degradation and addition, floc disintegration and coagulation, and aggregation-breakage processes in Taylor–Couette flow (see also [17–20]). In recent decades, a great deal of effort has been devoted to understanding the kinetics of coagulation–fragmentation processes [17–45]. Most intriguingly, many research works have shown that the size distribution of clusters in coagulation and coagulation–fragmentation systems can approach a scaling form in the long-time limit (see, e.g., [6–10, 26, 27, 45]). Moreover, an irreversible coagulation system always evolves permanently with time, while a reversible process can evolve to a steady state after a sufficiently long time [26, 36, 37]. In order to investigate analytically the dynamical evolution of coagulation–fragmentation processes, a useful rate-equation approach has been developed based on the mean-field assumption. Family *et al* studied aggregation–fragmentation processes by developing a scaling description for the cluster size distribution and determined the critical exponents based on the mean-field Smoluchowski rate equation, and they also testified the theoretical predictions by numerical simulations [26]. And Sorensen *et al* investigated the time evolution of the typical cluster size for the general case of coagulation with fragmentation [27], which is in good agreement with the simulation results done by Family *et al* [26]. Carr and da Costa discussed in detail asymptotic behavior of solutions to the coagulation–fragmentation equations in weak and strong fragmentation cases [31, 32]. Cañizo identified the equilibrium distribution to which solutions of the discrete coagulation–fragmentation system of equations converge for large times under the condition of detailed balance [37]. Li *et al* used distribution kinetics to model reversible aggregation and fragmentation processes, and they then obtained analytical and numerical simulation results for different aggregation and fragmentation rate kernels [38]. Straube and Falcke studied the kinetics of reversible aggregation and fragmentation with a periodically modulated binding rate [44]. In our previous work, we discussed the kinetics of aggregation processes with catalysis-driven fragmentation, in which two clusters of the same species bond spontaneously to form a large cluster while large clusters break up only with the help of a catalyst [45]. All these research works have made significant progress in the kinetics of coagulation–fragmentation processes.

As far as we know, most of research works have incorporated coagulation processes only with linear fragmentation. And only few investigations have been contributed to coagulation processes with fragmentation due to interactions between fragments, such as collision-induced fragmentation [20, 33, 39] and catalysis-driven fragmentation [45]. Collision-induced fragmentation may arise in practical cases including grinding and explosive-type processes. Krapivsky and Ben-Naim investigated the kinetics of nonlinear collision-induced fragmentation and obtained the explicit solution of the fragment size distribution [16]. Vigil *et al* considered a closed system of particles, in which any number of particles are produced by binary collisions, and they then studied the dynamical evolution of such coagulation processes with collision-induced breakage for arbitrary fragment distribution functions [39]. Coagulation with breakage due to particle–particle collisions may be important especially for systems with high dispersed-phase loadings [39]. On the other hand, collision-induced breakage (fragmentation) processes are intrinsically nonlinear [14–16], and studies of such processes can provide useful understanding of nonlinear effects in aggregation kinetics. Thus, it is of great practical and theoretical interest to probe into the kinetics of coagulation processes with collision-induced fragmentation.

Motivated by [16, 39], we have also investigated analytically the kinetics of coagulation processes with collision-induced fragmentation. Assume that there is only one species  $A$  in

the system and a cluster is characterized only by the number of its individual components. Two type- $A$  clusters can bond to form a larger cluster when they meet, which can be described as the reaction  $A_i + A_j \xrightarrow{I(i,j)} A_{i+j}$ . Here  $A_i$  denotes a cluster consisting of  $i$  monomers and  $I(i, j)$  denotes the reaction rate kernel at which two clusters coagulate together. Meanwhile, if a pair of clusters come across and destructively collide with each other, fragmentation of clusters arises. Cheng and Redner had thoroughly investigated the particular class of splitting models in which a two-particle collision results in three different outcomes: (i) both particles splitting exactly into two; (ii) only the larger particle splitting; or (iii) only the smaller particle splitting [14]. Moreover, in some situations a binary collision can produce a random amount of fragments [39] or result in clusters which are larger than the two colliding ones [1, 33]. For example, collisional breakage of an  $i$ -mer and a  $j$ -mer might yield a monomer and an  $(i + j - 1)$ -mer [33]. In this work, we focus only on another particular case, in which a randomly selected particle splits upon a binary collision while another particle remains intact [16]. Collision-induced fragmentation processes can be described by the formula  $A_l + A_{i+j} \xrightarrow{J(l;i,j)} A_l + A_i + A_j$ , where  $J(l; i, j)$  is the fragmentation rate kernel. Considering a semi-linear fragmentation kernel, we can obtain the explicit solution of the cluster size distribution. Intriguingly, the results show that the scaling properties of the cluster size distribution change qualitatively due to nonlinearities.

The paper is organized as follows. In section 2, we investigate the coagulation–fragmentation model by using the rate-equation approach and then analyze the scaling properties of the cluster size distribution. A brief summary is given in section 3.

## 2. Analytical solution of the coagulation–fragmentation model

The present investigation is based on the mean-field theory, which assumes that the reaction proceeds at a rate proportional to the concentrations of reactants. The mean-field approximation neglects spatial fluctuation of the reactant densities and therefore applies only to the case of the spatial dimension  $d$  equal to or greater than an upper critical dimension  $d_c$  [46, 47]. When  $d < d_c$ , fluctuations in the densities of reactants may lead to a dimension-dependent kinetic behavior in the long-time limit. Numerical simulations showed  $d_c = 2$  for irreversible aggregation processes [46]. But for reversible aggregation, Family *et al* verified that the mean-field rate-equation approach is valid for  $d \geq 1$  [26]. In this simplified reversible aggregation model, the aggregation rate and the fragmentation probability of any bond in clusters are constants independent of the cluster mass; hence, the upper critical dimension  $d_c$  for our model may be unity.

We assume that the spatial dimension of our system is  $d \geq 1$ . Fluctuations in the densities of reactants are ignored and the clusters are assumed to be homogeneously distributed throughout aggregation–fragmentation processes. Thus, the theoretical approach to such reversible aggregation processes can be based on the rate equations. At time  $t$ , the concentration of the clusters consisting of  $k$  monomers is denoted as  $a_k(t)$ . Based on the Smoluchowski rate equation given by Family *et al* [26], the governing rate equation of our model can be written as

$$\begin{aligned} \frac{da_k}{dt} = & \frac{1}{2} \sum_{i+j=k} I(i, j)a_i a_j - a_k \sum_{j=1}^{\infty} I(k, j)a_j \\ & + \sum_{l=1}^{\infty} \sum_{j=1}^{\infty} J(l; k, j)a_l a_{k+j} - \frac{1}{2} \sum_{l=1}^{\infty} \sum_{i+j=k} J(l; i, j)a_l a_{i+j}. \end{aligned} \tag{1}$$

In equation (1), the first two terms on the right-hand side account for the gain and loss in  $a_k(t)$  due to the coagulation processes  $A_i + A_{k-i} \rightarrow A_k$  and  $A_k + A_j \rightarrow A_{k+j}$  ( $i = 1, 2, \dots, k-1$  and  $j = 1, 2, 3, \dots$ ), respectively; while the last two terms account for the gain and loss in  $a_k(t)$  due to the collision-induced breakage processes  $A_l + A_{k+j} \rightarrow A_l + A_k + A_j$  and  $A_l + A_k \rightarrow A_l + A_i + A_{k-i}$  ( $l, j = 1, 2, 3, \dots$  and  $i = 1, 2, \dots, k-1$ ), respectively.

In this work, we aim to determine the explicit solution of the cluster size distribution  $a_k(t)$  from equation (1) and then investigate analytically the dynamical scaling properties of the coagulation–fragmentation system. However, since equation (1) with varying  $k$  is actually an infinite set of nonlinear differential equations, it is very difficult to determine straightforwardly the general analytical solution of  $a_k(t)$  for arbitrary kernels  $I(i, j)$  and  $J(l; i, j)$ . In the literature, some useful mathematical techniques have been developed to solve the nonlinear rate equations. For example, an approach based on the application of generating functions or Laplace transforms can be used to solve exactly the rate equation for irreversible coagulation processes with special kernels (see, e.g., [3, 8]). And another alternative approach is to make a scaling *ansatz* for the solution form of the rate equation, which is used extensively for coagulation processes with general rate kernels (see, e.g., [4, 6]); however, such an approach can provide only the asymptotical analytical solution of the cluster size distribution at large times. Moreover, in order to give a suitable scaling *ansatz* of the cluster size distribution for an unexplored system with general rate kernels, one should find out in advance the explicit solution of such a system with some special rate kernels. Here, we consider a simple chain-shaped cluster system with the special rate kernels  $I(i, j) = I$  and  $J(l; i, j) = 2Jl^u$  ( $I, J$  and  $u$  are all constants), which can be solved analytically. In the system, monomers can be connected together to form an open chain by breakable bonds, but the number of bonds of each monomer is not more than 2. So, there exist only chain-shaped clusters in our system. Obviously, each monomer within a  $k$ -mer ( $k > 1$ ) is connected to two nearest neighbors, except that the two monomers at the two ends of the chain are connected to only one nearest neighbor and have a dangling bond. Thus, a  $k$ -mer has two dangling bonds, which is independent of the value of  $k$ . And an isolated monomer has also two dangling bonds. In a reaction, only the reactants having dangling bonds are energetic and reactive, and the reaction rate may depend crucially on the number of the dangling bonds of each reactant. Hence, it is sound that for our system the coagulation rate between any two clusters is independent of their sizes, namely,  $I(i, j) \equiv I$ . Moreover, we assume that the interactions between any second- or higher-order nearest-neighbor monomers are all negligible compared with those between nearest neighbors and the bonds between any two nearest-neighbor monomers have the same breaking strength. Thus, in a collision, each bond within an arbitrary cluster has the same possibility of breakage, namely, the breakage rate  $J(l; i, j)$  at which an  $(i + j)$ -mer fragments into an  $i$ -mer and a  $j$ -mer is independent of the sizes  $i$  and  $j$ . It should also be pointed out that the breakage rate of an  $(i + j)$ -mer is directly proportional to the value of  $i + j - 1$  because a  $k$ -mer has exactly  $k - 1$  bonds. On the other hand, the breakage rate of a cluster may also have a relation with the impacting efficiency of the impacting cluster. In this model, a cluster is characterized only by its size (or equivalently, mass) and the impacting efficiency may be dependent on the size of the impacting cluster. In a spirit similar to [14], we also consider that the overall impacting efficiency of an  $l$ -mer can vary as  $l^u$  (here  $u$  is the homogeneity index). Thus, we get  $J(l; i, j) = 2Jl^u$  if the breakage rate of a bond is set to be  $J$ . Employing such particular rate kernels, we can determine the analytical solution of the cluster size distribution from equation (1). The study of the coagulation–fragmentation system with special rate kernels may provide a simple but useful step towards the theoretical understanding of nonlinear effect in aggregation kinetics.

With these hypotheses equation (1) can then be rewritten as

$$\frac{da_k}{dt} = \frac{I}{2} \sum_{i+j=k} a_i a_j - I M_0 a_k + 2J M_u \sum_{j=1}^{\infty} a_{k+j} - (k-1) J M_u a_k \quad (2)$$

with the short-hand notation  $M_u(t) = \sum_{k=1}^{\infty} k^u a_k(t)$ . Obviously, the zero- and first-order moments,  $M_0(t)$  and  $M_1(t)$ , are of concrete physical meaning.  $M_0(t)$  denotes the total number of clusters at time  $t$ , while  $M_1(t)$  describes the total size of clusters. Multiplying equation (2) with  $k$  and summing them up over all  $k$ , we obtain  $\dot{M}_1(t) = 0$ , with the exact solution  $M_1(t) \equiv M_1(0)$ . This indicates that the system formally obeys the mass conservation law. Now the problem reduces to determining the analytical solution of  $a_k(t)$  from equation (2).

### 2.1. The special case of $u = 1$

We first investigate the special case of  $u = 1$ . In order to deduce the analytical solution of equation (2) and then to discuss the kinetic evolution behavior of the system, we consider here a simplest but important case in which initially there only exist monomer clusters. The initial condition can be expressed as

$$a_k(0) = A_0 \delta_{k1}. \quad (3)$$

Under the monodisperse initial condition, equation (2) can be solved with the help of ansatz [48]

$$a_k(t) = A(t)[a(t)]^{k-1}. \quad (4)$$

Inserting equation (4) into equation (2), we can recast equation (2) into the following differential equations:

$$\frac{da}{dt} = \frac{I}{2} A - J A_0 a \quad \frac{dA}{dt} = -\frac{I A^2}{1-a} + 2J A_0 \frac{Aa}{1-a} \quad (5)$$

with the corresponding initial condition  $a(0) = 0$  and  $A(0) = A_0$ . It is worth noting that the mathematical technique employed above is a sort of the method of separation of variables under the condition  $0 < a(t) < 1$  for all  $t$ . Moreover, it should also be pointed out that an alternative approach based on the application of Laplace transforms may be useful to solve equation (2) in this special case (see, e.g., [8]).

From equation (5) we deduce

$$\frac{d \ln[A(1-a)^{-2}]}{dt} = 0 \quad (6)$$

which is straightforwardly solved to yield

$$A(t) = A_0 [1 - a(t)]^2. \quad (7)$$

Substituting equation (7) into equation (5), we obtain

$$\frac{da}{dt} = \frac{I}{2} A_0 a^2 - (I + J) A_0 a + \frac{I}{2} A_0. \quad (8)$$

Equation (8) can be readily solved to give the exact solution

$$a(t) = \frac{I(1 - e^{-C_2 t})}{I + J + C_1 - (I + J - C_1) e^{-C_2 t}} \quad (9)$$

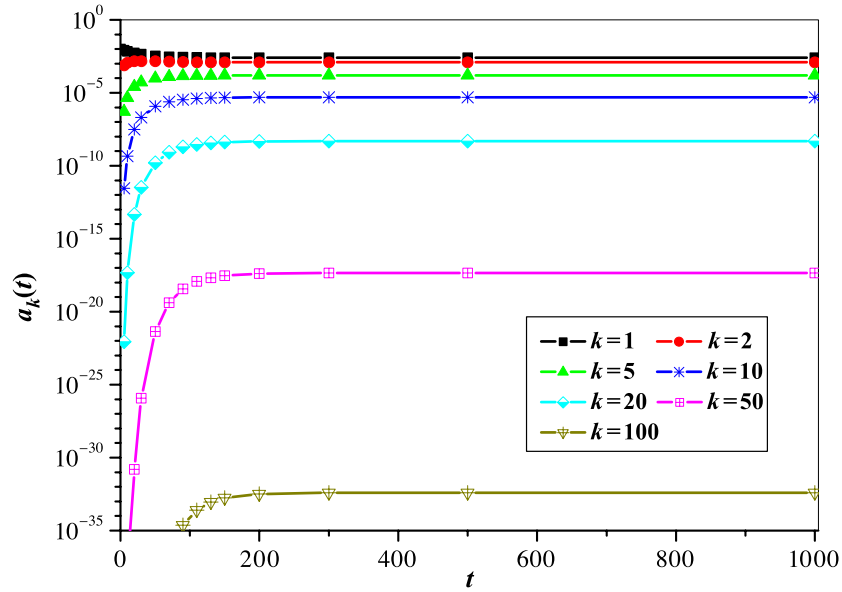


**Figure 1.** Semilog plot of the cluster size distribution  $a_k(t)$  versus time  $t$  for different size  $k$ . The initial condition is  $I = 4, J = 1, u = 1$  and  $A_0 = 0.01$ .

where  $C_1 = \sqrt{J^2 + 2IJ}$  and  $C_2 = C_1 A_0$ . Thus, we obtain the exact solution of the cluster size distribution as follows:

$$a_k(t) = A_0 \left[ \frac{J + C_1 - (J - C_1) e^{-C_2 t}}{I + J + C_1 - (I + J - C_1) e^{-C_2 t}} \right]^2 \left[ \frac{I(1 - e^{-C_2 t})}{I + J + C_1 - (I + J - C_1) e^{-C_2 t}} \right]^{k-1}. \tag{10}$$

In the region of  $t \gg 1$ , equation (10) can be asymptotically rewritten as

$$a_k(t) \simeq \frac{A_0(J + C_1)^2}{I(I + J + C_1)} \left( \frac{I}{I + J + C_1} \right)^k \exp[-kC_3 e^{-C_2 t}] \tag{11}$$

where  $C_3 = 2C_1/(I + J + C_1)$ .

The sketch of the time and size dependence of  $a_k(t)$  is shown in figure 1. It shows that the system will evolve to a steady state at  $t \rightarrow \infty$  and  $a_k(t)$  takes a nonzero steady-state distribution. Moreover, a plot of  $a_k(t)$  against  $k/\tilde{S}(t)$  can collapse the cluster size distributions for  $t \gg 1$ , where  $\tilde{S}(t) = [\ln(I + J + C_1) - \ln I + C_3 e^{-C_2 t}]^{-1}$ .  $\tilde{S}(t)$  is the typical size, which plays a role analogous to that of the correlation length in ordinary critical phenomena. Such a plot is illustrated in figure 2. It is not surprising because equation (11) can further be rewritten as  $a_k(t) \sim \exp[-k/\tilde{S}(t)]$ .

The result shows that for this case the cluster size distribution takes the modified scaling form [43],

$$a_k(t) \sim \lambda^k [f(t)]^{-w} \Phi[k/S(t)] \quad S(t) \propto [f(t)]^z. \tag{12}$$

Here,  $f(t)$  is a monotonically increasing function of time. And the governing scaling exponents,  $w$  and  $z$ , describe the scaling properties of the cluster size distribution. In this case,  $f(t) = e^t$ ,  $w = 0$  and  $z = C_2$ . Moreover, the modified scaling form of equation (12) implies that there are two scales, the growing scale  $S(t) \propto [f(t)]^z$  and the time-independent

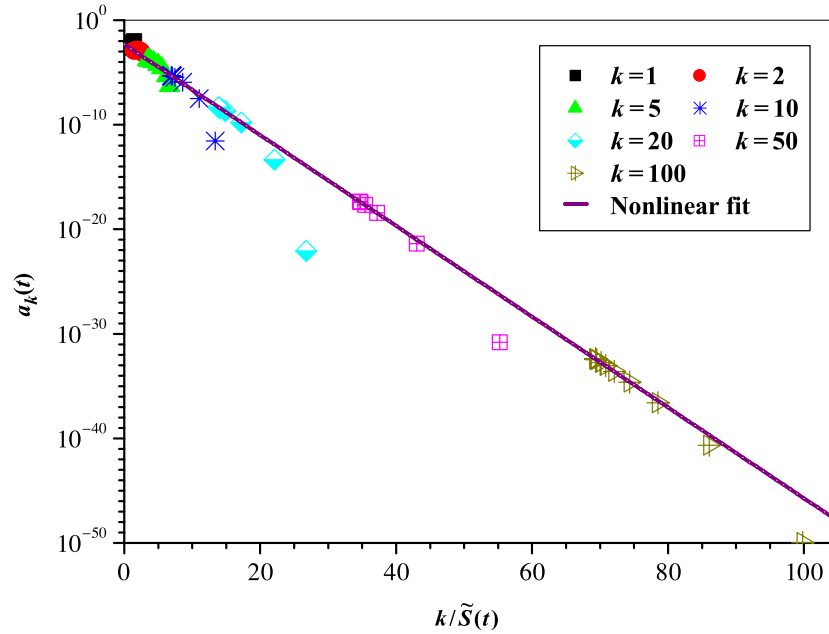


**Figure 2.** Semilog plot of the cluster size distribution  $a_k(t)$  versus rescaled size  $k/\tilde{S}(t)$ , where  $\tilde{S}(t) = [\ln(I + J + C_1) - \ln I + C_3 e^{-C_2 t}]^{-1}$ . The initial condition is  $I = 4, J = 1, u = 1$  and  $A_0 = 0.01$ .

scale  $S = \lim_{t \rightarrow \infty} M_2(t)/M_1(t) \simeq (1 + \lambda)/(1 - \lambda)$ , associated with  $a_k(t)$ . This is different from the conventional scaling law only with a single scale (see, e.g., [48]). For this case, the typical size is  $\tilde{S}(t) = [\ln(S + 1) - \ln(S - 1) + 1/S(t)]^{-1}$ . Obviously, the time-independent scale will dominate the large-time evolution behavior of the cluster size distribution.

Moreover, the total number of clusters is  $M_0(t) = A_0[J + C_1 - (J - C_1)e^{-C_2 t}][I + J + C_1 - (I + J - C - 1)e^{-C_2 t}]^{-1}$ . This indicates that the total number can remain a certain value in the long-time limit. Hence, after a sufficiently long time, a balance will be established between coagulation and collision-induced breakage processes, and the cluster size distribution will take a nonzero steady-state scaling form finally (namely, small-size clusters can always coexist with large-size ones). In this special case, our model has the same evolution properties as coagulation processes with linear fragmentation studied in [24–26, 31, 32, 37].

### 2.2. The special case of $u = 0$

We then turn to another special case of  $u = 0$ . Under the monodisperse initial condition, equation (2) can also be analytically solved with the help of ansatz (4). Substituting equation (4) into equation (2), we deduce two differential equations for this case,

$$\frac{da}{dt} = \frac{I}{2}A - J\frac{Aa}{1-a} \quad \frac{dA}{dt} = -\frac{IA^2}{1-a} + 2J\frac{A^2a}{(1-a)^2}. \tag{13}$$

Employing the same algebra used in the above case, we solve equation (13) and then obtain the exact solution of the cluster size distribution as follows:

$$a_k(t) = \frac{4A_0J^2}{(I + 2J - Ie^{-JA_0t})^2} \left[ \frac{I(1 - e^{-JA_0t})}{I + 2J - Ie^{-JA_0t}} \right]^{k-1}. \tag{14}$$



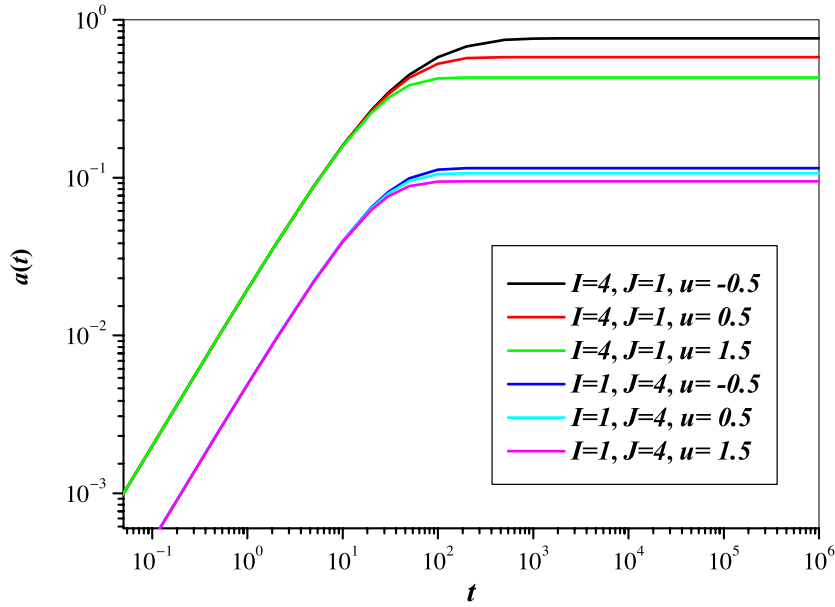


**Figure 3.** Log–log plot of  $a(t)$  versus time  $t$  for different values of the parameters  $I, J$  and  $u$ . The initial concentration of monomers is the same for all numerical computations,  $A_0 = 0.01$ .

In the long-time limit, equation (14) can be asymptotically rewritten as

$$a_k(t) \simeq \frac{4A_0J^2}{I(I+2J)} \left( \frac{I}{I+2J} \right)^k \exp[-k/S(t)] \quad S(t) = \frac{I+2J}{2J} e^{JA_0t} \quad (15)$$

which satisfies the modified scaling form of equation (12). For this case, the growing scale is  $S(t) \propto e^{JA_0t}$  while the time-independent scale is  $S = (I + J)/J$ . Moreover, the total number of clusters can remain a constant value  $2JA_0/(I + 2J)$  at large times. Similar to the above-discussed case of  $u = 1$ , the system in this case will also evolve to a steady state after a sufficiently long time.

### 2.3. The general case of $u \geq -1$

We now investigate the general case of  $u \geq -1$ . Analyzing the results of the above special cases, we can also make ansatz (4) for equation (2) in general cases under the monodisperse initial condition. Obviously, equation (7) also holds in general cases. Substituting equations (4) and (7) into equation (2), we obtain the following differential equation:

$$\frac{da}{dt} = \frac{A_0}{2}(1-a)^2 \left( I - 2J \sum_{k=1}^{\infty} k^u a^k \right). \quad (16)$$

The solution of  $a(t)$  depends crucially on the value of  $u$  as well as the coefficients ( $I$  and  $J$ ) of the rate kernels. It is very difficult to determine the exact explicit expression of  $a(t)$  from equation (16) in general cases. When the parameters ( $A_0, I, J$  and  $u$ ) are all given, one may obtain the numerical solution of  $a(t)$  by numerical computation of equation (16). Some examples are illustrated in figure 3. Here, we will focus only on the explicit scaling solution of the cluster size distribution at large times.

It follows from equation (16) that either  $a(t) \rightarrow 1$  or  $2J \sum_{k=1}^{\infty} k^u [a(t)]^k \rightarrow I$  at  $t \rightarrow \infty$ . Moreover,  $I - 2J \sum_{k=1}^{\infty} k^u [a(t)]^k$  must be equal to or greater than zero so as to ensure  $\dot{a}(t) \geq 0$ . On the other hand, ansatz (4) implies that  $0 < a(t) < 1$  should be obeyed for all time  $t > 0$ . Thus, we can conclude that  $a(\infty) \rightarrow 1$  in the  $I \geq 2J \sum_{k=1}^{\infty} k^u$  case and  $a(\infty) \rightarrow a_{\infty}$  in the remaining case ( $a_{\infty}$  is a finite constant satisfying the equation  $I = 2J \sum_{k=1}^{\infty} k^u a_{\infty}^k$  and  $0 < a_{\infty} < 1$ ). It is obvious that  $\sum_{k=1}^{\infty} k^u \rightarrow \infty$  and  $I < 2J \sum_{k=1}^{\infty} k^u$  in the  $u \geq -1$  case. Thus, we can deduce  $a(t) \rightarrow a_{\infty}$  at  $t \rightarrow \infty$ . This can be verified by the results of numerical computations illustrated in figure 3. In the continuum limit, we find  $a_{\infty} \simeq \exp\{-[2JI^{-1}\Gamma(u+1)]^{1/(u+1)}\}$  for  $u > -1$ . Especially, one can exactly determine  $a_{\infty} = 1 - e^{-I/2J}$  for  $u = -1$ .

In the long-time limit, we introduce a new variable  $\tilde{a}(t) = a_{\infty} - a(t)$  and then recast equation (16) into an asymptotical linearized equation as follows:

$$\frac{d\tilde{a}}{dt} \simeq -\gamma\tilde{a} \tag{17}$$

where  $\gamma = JA_0(1 - a_{\infty})^2 \sum_{k=1}^{\infty} k^{u+1} a_{\infty}^{k-1}$ . Equation (17) is easily solved to give

$$\tilde{a}(t) \simeq C_4 e^{-\gamma t} \tag{18}$$

where  $C_4$  is an integration constant. Making use of equations (18) and (7), we then obtain the large-time explicit expression of the cluster size distribution as follows:

$$a_k(t) \simeq A_0(1 - a_{\infty})^2 a_{\infty}^k \exp[-k/S(t)] \quad S(t) = a_{\infty} C_4^{-1} e^{\gamma t} \tag{19}$$

which takes the modified scaling form of equation (12), with the typical size  $\tilde{S}(t) = [-\ln a_{\infty} + C_4 a_{\infty}^{-1} e^{-\gamma t}]^{-1}$ .

The above linearization method is a classical approach to study the asymptotical solutions of nonlinear differential equations near the equilibrium point. Such a technique may be fairly useful to investigate our coagulation–fragmentation model with general rate kernels. Provided the given rate kernels can ensure that collision-induced breakage of clusters dominates over or at least balances against coagulation of clusters, our system will eventually evolve to a steady state and equation (1) can be approximated as a series of linearized equations for the cluster size distribution near the equilibrium point. These investigations will be deferred to a future work.

In this general case, a balance can always be established between coagulation and collision-induced breakage processes and the cluster size distribution can evolve to a steady-state scaling form finally. Based on the numerical computation results of equation (16), one can also obtain the numerical solution of the cluster size distribution in the system with given parameters (see, e.g., figure 4). Figure 4 shows that a plot of  $a_k(t)$  against a suitable rescaled size does collapse the cluster size distributions for  $k \gg 1$  and  $t \gg 1$ , which can verify our analytical results above.

#### 2.4. The general case of $u < -1$

Finally, we investigate the general case of  $u < -1$ . Differential equation (16) of  $a(t)$  also holds in this general case. Obviously,  $\sum_{k=1}^{\infty} k^u$  has a finite value for  $u < -1$ . Let  $\zeta(x)$  be the Riemann zeta function,  $\zeta(x) = \sum_{k=1}^{\infty} k^{-x}$  ( $x > 1$ ). The solution of equation (16) further depends on the relation between the values  $\zeta(-u)$  and  $I/2J$ . We then investigate the kinetic behavior of the system in three distinct subcases.

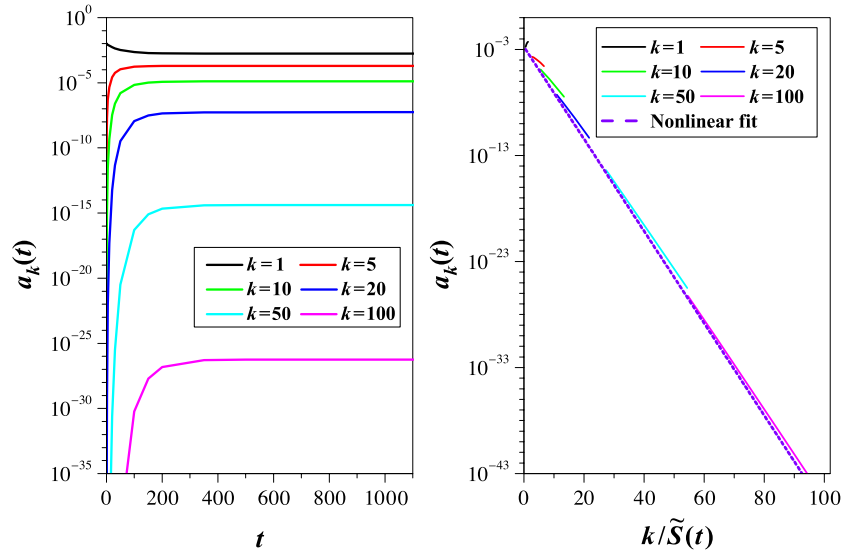


**Figure 4.** (i) Left plot: semilog plot of the cluster size distribution  $a_k(t)$  versus time  $t$  for different size  $k$ . (ii) Right plot: semilog plot of  $a_k(t)$  versus rescaled size  $k/\tilde{S}(t)$  for  $20 < t < 50000$ , where  $\tilde{S}(t) = \ln^{-1}[1/a(t)]$ . The initial condition for numerical computations is  $I = 4, J = 1, u = 0.5$  and  $A_0 = 0.01$ .

2.4.1.  $I < 2J\zeta(-u)$  subcase. In this subcase, from equation (16) we again deduce the following asymptotical solution of  $a(t)$  in the long-time limit:

$$a(t) \simeq a_\infty - C_4 e^{-\gamma t} \tag{20}$$

which is the same as that obtained in the above case of  $u \geq -1$ . Thus, the solution of the cluster size distribution in this subcase is the same as equation (19), and the system can also evolve to a steady state finally.

2.4.2.  $I = 2J\zeta(-u)$  subcase. In this special subcase, we solve equation (16) and then obtain the asymptotical solution as follows:

$$a(t) \simeq \begin{cases} 1 - C_5 t^{1/u} & \text{for } -1 > u > -2 \\ 1 - C_6 (t \ln t)^{-1/2} & \text{for } u = -2 \\ 1 - C_7 t^{-1/2} & \text{for } u < -2 \end{cases} \tag{21}$$

where  $C_5 = 2[-4JA_0u\Gamma(2+u)]^{1/u}$ ,  $C_6 = (JA_0)^{-1/2}$  and  $C_7 = [2JA_0\zeta(-u-1)]^{-1/2}$ . By using equation (21) we determine the asymptotical solution of the cluster size distribution in the long-time limit,

$$a_k(t) \simeq \begin{cases} A_0 C_5^2 t^{2/u} \exp(-C_5 k t^{1/u}) & \text{for } -1 > u > -2 \\ A_0 C_6^2 (t \ln t)^{-1} \exp[-C_6 k (t \ln t)^{-1/2}] & \text{for } u = -2 \\ A_0 C_7^2 t^{-1} \exp(-C_7 k t^{-1/2}) & \text{for } u < -2. \end{cases} \tag{22}$$

Equation (22) shows that each  $a_k(t)$  ( $k > 1$ ) increases with time first, then reaches a peak value, and finally decays to zero (see, also, figure 5).

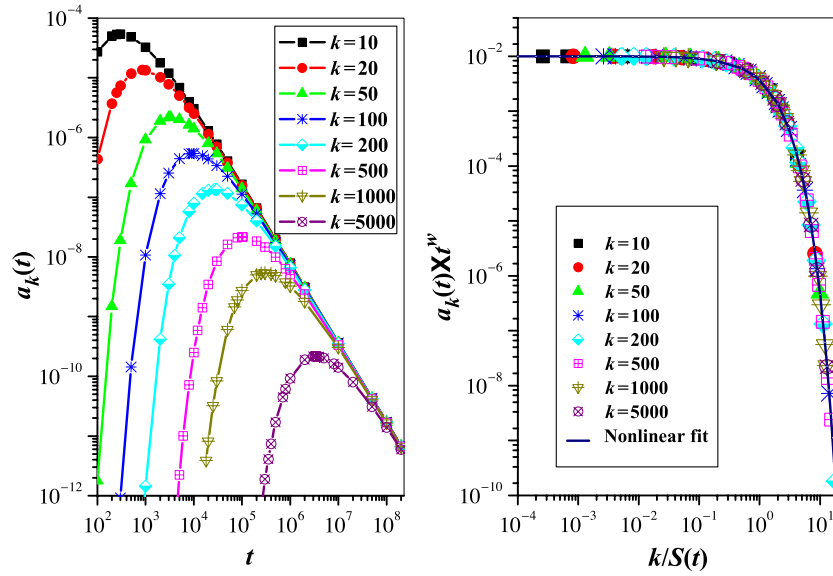


**Figure 5.** (i) Left plot: log–log plot of the cluster size distribution  $a_k(t)$  versus time  $t$  for different size  $k$ . (ii) Right plot: log–log plot of  $a_k(t) \times t^w$  versus rescaled size  $k/S(t)$ , where  $w = -2/u$  and  $S(t) = t^{-1/u}$ . The initial condition is  $I = 5.225$ ,  $J = 1$ ,  $u = -1.5$  and  $A_0 = 0.01$ .

On the other hand, equation (22) also indicates that the cluster size distribution in this special subcase ( $u < -1$  and  $u \neq -2$ ) can obey the conventional scaling form [48]

$$a_k(t) \sim t^{-w} \Phi[k/S(t)] \tag{23}$$

with only the growing scale  $S(t) \propto t^z$ . It follows from equation (23) that a plot of  $a_k(t) \times t^w$  against  $k/S(t)$  can collapse the cluster size distributions for all  $k \gg 1$  and  $t \gg 1$ . Such a plot is shown in figure 5. Figure 5 indicates that the growing scale  $S(t)$  in equation (23) plays the same role as  $\tilde{S}(t)$  introduced in the special  $u = 1$  case. So, the growing scale  $S(t)$  is just the typical size for the conventional scaling law. As for the special subcase of  $u = -2$ , the cluster size distribution takes the logarithm-correction scaling form of equation (23),  $a_k(t) \sim (t \ln t)^{-w} \Phi[k/S(t)]$ , with the growing scale  $S(t) \propto (t \ln t)^z$ .

It is well known that the typical size in an irreversible coagulation system is  $S(t) \propto t$  (see, e.g., [48]). In this subcase, the scaling exponent  $z$  is always smaller than 1. Thus, the growing rate of the typical size  $S(t)$  in this subcase is lower than that in irreversible coagulation cases. This shows that the coagulation course of clusters can be prolonged by collision-induced fragmentation.

It is also instructive to determine the total number of clusters,

$$M_0(t) \simeq \begin{cases} A_0 C_5 t^{1/u} & \text{for } -1 > u > -2 \\ A_0 C_6 (t \ln t)^{-1/2} & \text{for } u = -2 \\ A_0 C_7 t^{-1/2} & \text{for } u < -2. \end{cases} \tag{24}$$

The results show that the total number in this subcase always decays with time and decreases to zero in the end. Hence, the system will evolve permanently in time and all the monomers will bond together to form one giant cluster finally. In other words, coagulation of clusters will dominate over collision-induced breakage of clusters in the long-time limit.

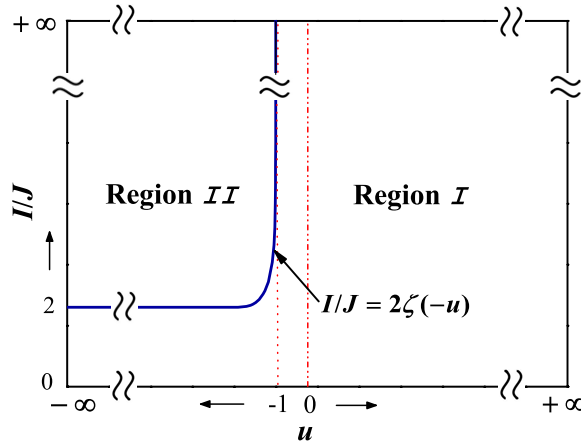


**Figure 6.** Diagrammatic sketch of the regions of two different scaling regimes. (i) Region I: the cluster size distribution satisfies the modified scaling law. (ii) Region II: the cluster size distribution satisfies the conventional scaling law. The two regions are divided by the curve of  $I/J = 2\zeta(-u)$ .

2.4.3.  $I > 2J\zeta(-u)$  subcase. In this subcase, equation (16) can be solved to yield the large-time asymptotical solution

$$a(t) \simeq 1 - C_8 t^{-1} \tag{25}$$

where  $C_8 = 2A_0^{-1}[I - 2J\zeta(-u)]^{-1}$ . One then readily deduces the scaling solution of  $a_k(t)$  at large times,

$$a_k(t) \simeq A_0 C^2 C_8 t^{-2} \exp(-C_8 k t^{-1}) \tag{26}$$

which also takes the conventional scaling form of equation (23), with the universal scaling exponents  $w = 2$  and  $z = 1$ . Equation (26) shows that the cluster size distribution in this subcase is similar to that in irreversible coagulation processes. Hence, in the long-time limit, collision-induced breakage of clusters is negligible and the evolution of the system is controlled crucially by coagulation of clusters.

### 3. Summary

We have proposed a single-species coagulation model with collision-induced fragmentation. In the system, when a pair of clusters come across, they can coagulate to form a larger one due to a complete inelastic collision; meanwhile, one and only one of them may fragment into two smaller clusters if the collision is elastic and destructive. We then investigated a simple but solvable system, in which the coagulation reaction kernel is constant and the fragmentation kernel is size-dependent, namely,  $I(i, j) = I$  and  $J(l; i, j) = 2Jl^u$ , and the initial size distribution of clusters is  $a_k(0) = A_0\delta_{k1}$ . The analytical solution of the cluster size distribution was deduced by means of the rate-equation approach. It was found that the results are crucially dependent on the value of index  $u$ .

When  $u \geq -1$ , a balance can always be established between coagulation and collision-induced breakage processes, and the system can evolve to a steady state eventually. The cluster size distribution  $a_k(t)$  takes the modified scaling form of equation (12) and the total number keeps a nonzero constant in the long-time limit. Moreover, clusters of any size can coexist in the system throughout the processes. Especially, one can obtain the exact solution of  $a_k(t)$  in

the special  $u = 0$  and  $u = 1$  cases, which can verify the analytical results for the general case of  $u \geq -1$ .

When  $u < -1$ , the kinetic behavior of the system further depends on the relation between the values  $I$  and  $2J\zeta(-u)$ . For  $I < 2J\zeta(-u)$ ,  $a_k(t)$  also takes the modified scaling form of equation (12) and the evolution property of this system is similar to that of the above-mentioned  $u \geq -1$  case. For  $I \geq 2J\zeta(-u)$ ,  $a_k(t)$  approaches the conventional scaling form of equation (23), and the total number decreases with time and decays consistently to zero in the end; hence, the system will evolve permanently in time. So, it can be concluded that for the case of  $u < -1$  and  $I \geq 2J\zeta(-u)$ , the evolution of the system is controlled crucially by coagulation of clusters while collision-induced fragmentation of clusters can only prolong the evolution course.

In short, the cluster size distribution in coagulation and collision-induced fragmentation processes with the special rate kernels  $I(i, j) = I$  and  $J(l; i, j) = 2Jl^u$  may evolve according to either of the scaling regimes: the modified form or the conventional form. And the two different regions are divided by the curve of  $I = 2J\zeta(-u)$ , as shown in figure 6. As for our model with general rate kernels, more sophisticated mathematical methods may be required to determine the explicit solution of the cluster size distribution.

## Acknowledgments

This work was supported by the National Natural Science Foundation of China under grant nos. 10775104 and 10305009. XS thanks the support from Chinese National Science Foundation (10725418) and Ground Fund of Shanghai Science and Technology Foundation (05DJ14003).

## References

- [1] Safronov V S 1972 *Evolution of the Protoplanetary Cloud and Formation of the Earth and the Planets* (Jerusalem: Israel Program for Scientific Translations)
- [2] Silk J 1980 *Star Formation* (Switzerland: Geneva Observatory, Sauverny)
- [3] Family F and Landau D P 1984 *Kinetics of Aggregation and Gelation* (Amsterdam: North-Holland)
- [4] Meakin P 1992 *Rep. Prog. Phys.* **55** 157
- [5] Vicsek T and Family F 1984 *Phys. Rev. Lett.* **52** 1669
- [6] van Dongen P G J and Ernst M H 1985 *Phys. Rev. Lett.* **54** 1396
- [7] Kang K, Redner S, Meakin P and Leyvraz F 1986 *Phys. Rev. A* **33** 1171
- [8] Menon G and Pego R L 2004 *Commun. Pure Appl. Math.* **57** 1197
- [9] Menon G and Pego R L 2005 *SIAM J. Math. Anal.* **36** 1629
- [10] Fournier N and Laurençot P 2005 *Commun. Math. Phys.* **256** 589
- [11] Blatz P J and Tobolsky A V 1945 *J. Phys. Chem.* **49** 77
- [12] Habib P 1983 *An Outline of Soil and Rock Mechanics* (Cambridge: Cambridge University Press)
- [13] Ziff R M and McGrady E D 1986 *Macromolecules* **19** 2513
- [14] Cheng Z and Redner S 1990 *J. Phys. A: Math. Gen.* **23** 1233
- [15] Kostoglou M and Karabelas A J 2000 *J. Phys. A: Math. Gen.* **33** 1221
- [16] Krapivsky P L and Ben-Naim E 2003 *Phys. Rev. E* **68** 021102
- [17] McCoy B J and Madras G 1998 *J. Colloid Interface Sci.* **201** 200
- [18] Wang L, Vigil R D and Fox R O 2005 *J. Colloid Interface Sci.* **285** 167
- [19] Wang L, Marchisio D L, Vigil R D and Fox R O 2005 *J. Colloid Interface Sci.* **282** 380
- [20] Fasano A, Rosso F and Mancini A 2006 *Physica D* **222** 141
- [21] Barrow J D 1981 *J. Phys. A: Math. Gen.* **14** 729
- [22] van Dongen P G J and Ernst M H 1984 *J. Stat. Phys.* **37** 301
- [23] Kolb M 1986 *J. Phys. A: Math. Gen.* **19** L263
- [24] Cohen R J and Benedek G 1982 *J. Phys. Chem.* **86** 3696
- [25] Ziff R M and McGrady E D 1985 *J. Phys. A: Math. Gen.* **18** 3027
- [26] Family F, Meakin P and Deutch J M 1986 *Phys. Rev. Lett.* **57** 727

- [27] Sorensen C M, Zhang H X and Taylor T W 1987 *Phys. Rev. Lett.* **59** 363
- [28] Shih W Y, Aksay I A and Kikuchi R 1987 *Phys. Rev. A* **36** 5015
- [29] Vigil R D and Ziff R M 1989 *J. Colloid Interface Sci.* **133** 257
- [30] Oshanin G S and Burlatsky S F 1989 *J. Phys. A: Math. Gen.* **22** L973
- [31] Carr J 1992 *Proc. R. Soc. Edinb. A* **121** 231
- [32] Carr J and da Costa F P 1994 *J. Stat. Phys.* **77** 89
- [33] Laurençot P and Wrzosek D 2001 *J. Stat. Phys.* **104** 193
- [34] Madras G and McCoy B J 2002 *J. Colloid Interface Sci.* **246** 356
- [35] Escobedo M, Mischler S and Perthame B 2002 *Commun. Math. Phys.* **231** 157
- [36] Niethammer B 2003 *J. Nonlinear Sci.* **13** 115
- [37] Cañizo J A 2007 *J. Stat. Phys.* **129** 1
- [38] Li R, McCoy B J and Diemer R B 2005 *J. Colloid Interface Sci.* **291** 375
- [39] Vigil R D, Vermeersch I and Fox R O 2006 *J. Colloid Interface Sci.* **302** 149
- [40] Blackman J A and Marshall A 1994 *J. Phys. A: Math. Gen.* **27** 725
- [41] Gimel J C, Nicolai T and Durand D 2001 *Eur. Phys. J. E* **5** 415
- [42] Diemer R B and Olson J H 2002 *Chem. Eng. Sci.* **57** 2193
- [43] Ke J, Cai X O and Lin Z 2004 *Phys. Lett. A* **331** 281
- [44] Straube R and Falcke M 2007 *Phys. Rev. E* **76** 010402
- [45] Ke J, Wang X, Lin Z and Zhuang Y 2004 *Physica A* **338** 356
- [46] Kang K and Redner S 1984 *Phys. Rev. A* **30** 2833
- [47] Vicsek T, Meakin P and Family F 1985 *Phys. Rev. A* **32** 1122
- [48] Krapivsky P L 1993 *Physica A* **198** 135